Transient Analysis of Interconnect Networks Characterized by Measured Scattering-Parameter Data

Jimmy Shinn-Hwa Wang
Wayne Wei-Ming Dai

Baskin Center for
Computer Engineering & Information Sciences
University of California, Santa Cruz
Santa Cruz, CA 95064 USA

ABSTRACT

This paper describes a novel approach for incorporating the components characterized by the measured scattering-parameter (S-parameter) data into an S-parameter macromodel based simulator. This approach first converts the measured S-parameter data into frequency-dependent parasitic functions: $R(f)$, $L(f)$, $C(f)$, and $G(f)$, which are later used to compute the moments of the S-parameter for the construction of the macromodel. Benefiting from the weak frequency dependency nature of the $R(f)$, $L(f)$, $C(f)$, and $G(f)$ functions, this method allows the moments to be calculated in a much more accurate fashion than those obtained from fitting the S-parameter directly. This method also has several added advantages such as: the moments produced are independent of the approximation order and insensitive to measurement errors, furthermore, they observe power conservation rule for passive systems. The simulation results show very good agreements with the results produced by the direct convolution approach.

Keywords: Measured Data, Scattering Parameter, S-Parameter, Transient Analysis, Measured S-Parameter, Tabulated S-Parameter, Macromodel, S-Parameter Based Macromodel Simulator, Frequency-Dependent Parasitic

Contents

1   Introduction

Interconnect design has become an important issue in the high performance systems due to the recent advance in the packaging technology. As the packaging density and the clock speed of the Integrated Circuit (IC) increase, the frequency-dependent losses as well as the crosstalk induced noise have become some of the major issues in the designs of the interconnect networks. Due to the high switching speed of today's digital system, the magnitudes of the harmonics of the transmitted signals above 1 GHz can often become the significant components in the power spectrum. At these high frequencies, the interconnects exhibit more frequency-dependent conductor (skin effect) and the dielectric losses. The electro-static field solution can no longer predict the correct parasitics for the interconnects that carry the high-speed digital signals. The correct modeling of the transmission lines requires accurate modeling of both the frequency-dependent conductor (skin effect) and the dielectric losses. The measured S-parameter data can easily capture the behavior of these losses. The discontinuities in interconnects are difficult to describe with close form equations; they are better characterized with the measured S-parameter data. As a result, an accurate and a more efficient circuit simulator which can accept devices characterized with measured S-parameter data is necessary for the design of advanced packaging.

Integrating the measured models into a moment matching simulator is a problem because derivatives of the frequency dependent measured data which are required to generate the moments are not available explicitly. Generating the required moments using a numerical differentiation can often lead to large computation errors [15]. Since the information necessary for the construction of the scattering parameter macromodel does not exist explicitly, a novel method for retrieving the information needed must be developed with special attentions must be paid to avoid the numerical instabilities.

Gruodis et al. has previously reported the measurements of the admittance matrix $\mathbf{Y}_{2n}$ and the impedance matrix $\mathbf{Z}_{2n}$ of the transmission lines, the computation of the $\mathbf{Y}_0$ matrix propagation constant Γ, and the simulation using the state variable transfer function method [9]. The deficiency associated with Gruodis' method was the fact that the admittance matrix $\mathbf{Y}_{2n}$ and the impedance matrix $\mathbf{Z}_{2n}$ were difficult to measure at a frequency above several MHz which is specifically stated in Gruodis et al. paper [9]. Unlike the impedance matrix $\mathbf{Z}_{2n}$ and the admittance matrix $\mathbf{Y}_{2n}$ which

may not exist for the cases of the serial circuits or shunt circuits respectively, the S-parameter matrix always exists for any physical circuits [15] [17]. So the choice is to measure the S-parameter data for the transient simulation. Sanaie et al. used the balance-reduction method [15] and Miguel Silveria et al. utilized the curve-fitting of the transfer function section-by-section [17]. Kuznetsov et al. used the direct rational function curve-fitting of the wave propagation function [11]. All of them try to extract information from the curve-fitting of the S-parameter data directly. Since the S-parameter data are strong functions of frequency, the direct approach is very difficult. Thus Miguel Silveria et al. suggested to perform the curve-fitting section-by-section with each section no larger than a decade. Although accurate, this section-by-section method generates more information than necessary. This leads to Miguel Silveria's proposal to use a balance-reduction method to reduce the order. Chang et al. has implemented a direct convolution method into the HP Spice [18]. This method requires the impulse response found from inverse Fast Fourier Transform (IFFT) of the measured S-parameter data. Chang et al. further improves their method using direct fitting of the measured data with a rational function [4]. Hu et al. has incorporated the recursive convolution method into SWEC [10]. This method also calls for the impulse response found through IFFT. The drawback of convoluting the impulse response is the assumption of the relations between the real part and the imaginary part of all the S-parameters. The implementation usually requires the data of the imaginary part to be thrown away, whereas the Gruodis method of converting the measured S-parameter data into the parasitic functions makes use of all the data on hand.

The purpose of this paper is to propose an indirect method of finding the moments from the measured S-parameter data. The novel indirect method of computing the moments calls for a conversion of the S-parameter data into the parasitic functions before finding the Taylor series expansions. After the S-parameters has been converted into the parasitic functions, $\mathbf{R}(f)$, $\mathbf{L}(f)$, $\mathbf{C}(f)$ and $\mathbf{G}(f)$, a Least-Square curve-fitting of the S-parameter computed from these four data sets with respect to the measured S-parameter data is issued in order to find the moments of these four parasitic functions. The exact moments of the S-parameter functions are subsequently computed from the moments of these four parasitic functions. Based on the exact moments found using the indirect approach, the macromodel of transmission lines characterized with frequency-dependent losses is constructed and the transient simulation is performed.

The motivation of taking this indirect approach is shown in Section 2. The general steps of this

novel indirect approach will be presented in Section 3, whereas in Section 4, two methods to convert the measured S-parameter data into the parasitic functions will be shown. Section 5 will present the algorithm for the finding of the moments of the parasitic functions through indirect curve-fitting method. Section 6 will demonstrate the approach of how to construct the S-parameter macromodel from the moments of the parasitic functions. The experimental results will be presented in Section 7 and the conclusion will be addressed in Section 8.

2   Motivations

One cannot emphasis enough the advantages of finding the moments of the S-parameters from this algorithm. The followings are the most compelling reasons for this indirect approach: The
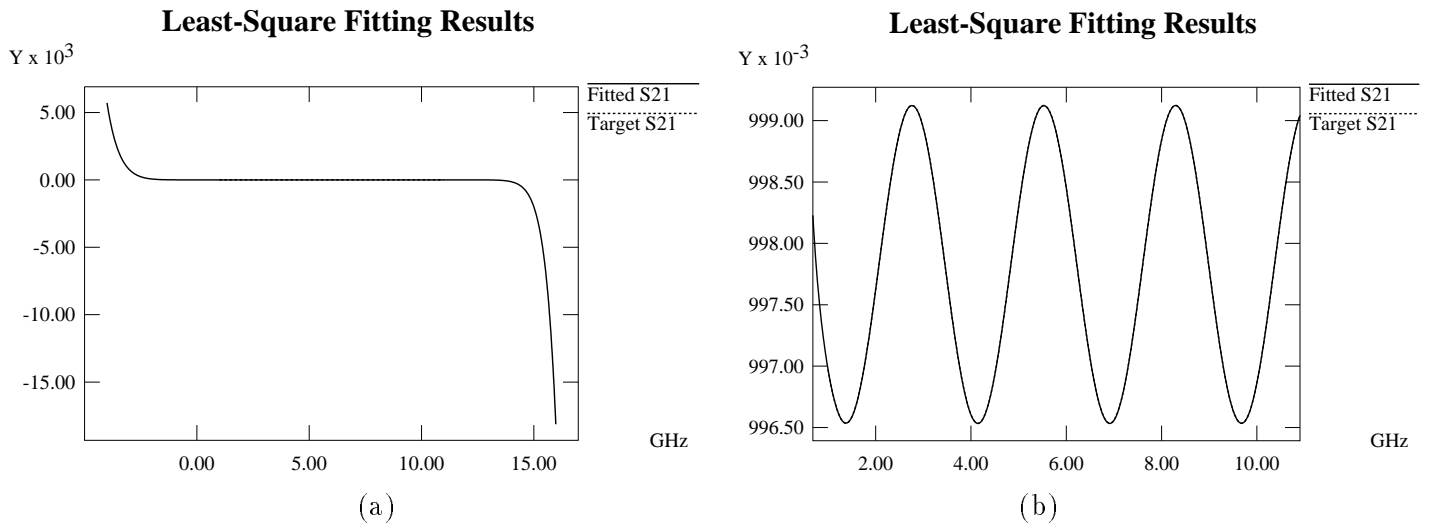

Figure 2.1: **A Particular Curve-Fitting Example:** The curves in (a) is plotted against extended frequency range beyond the sampled frequency spectrum. The curves in (b) is plotted against only the sampled frequency spectrum which spans from 1.0 GHz to 11.5 GHz.

computed S-parameter curves demonstrate the periodical nature not only within the spectrum of the measurements but also in the spectra above and below. This is not true for other methods which do curve-fitting the measured S-parameters directly. For example, the Root-Mean-Square (RMS) error for the Least-Square curve-fitting within the sampling spectrum could be very small, but can be unbounded outside of the sampling spectrum. Figure 2.1 (a) shows a particular example
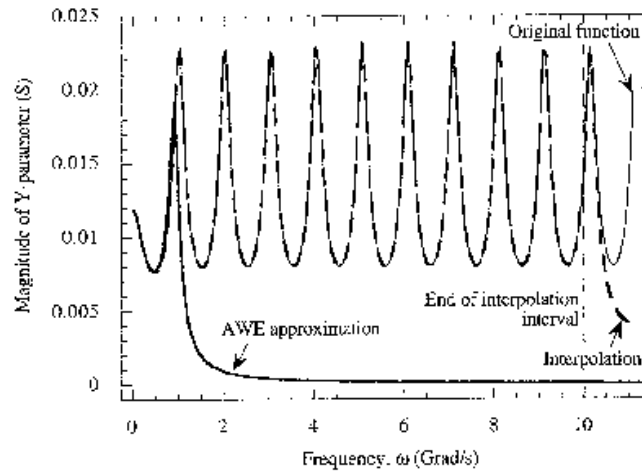
Figure 2.2: **AWEsim and Rational function Curve-Fitting Comparison:** AWEsim is proven inadequate to be used in curve-fitting and interpolation. Direct fitting to rational function is good only to be used as interpolation tool.
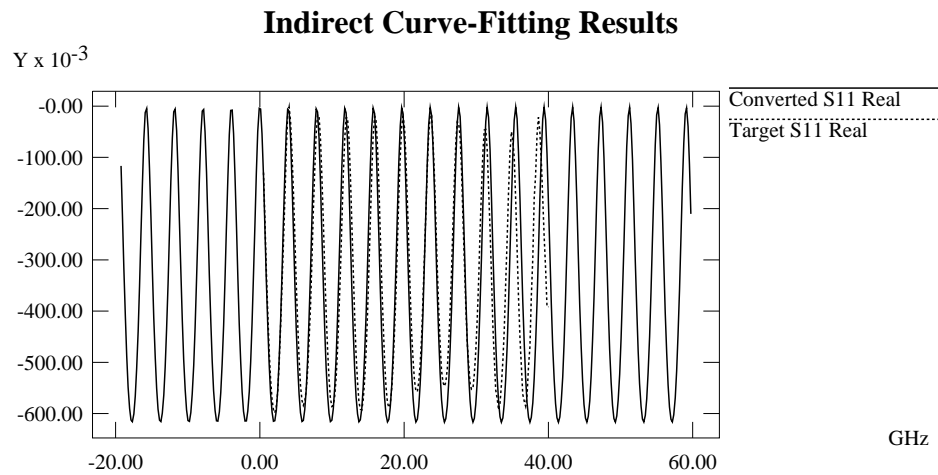

Figure 2.3: **Indirect Curve-Fitting Example:** The indirect method produces bounded and periodical computed S-parameter data both inside and outside of the sampling spectrum which spans from 0.5 GHz to 40.5 GHz. It is good both as an interpolation and extrapolation tool.

where the RMS error of the Least-Square curve-fitting equals to 0.0245 and the resulting function is unbounded outside of the sampled spectrum. Figure 2.1 (b) shows how well the least-square curve-fitting performs over the sampled spectrum. Figure 2.2 shows the AWEsim fitting characteristic and the direct rational function fitting results [12]. AWEsim is not suitable for the fitting to functions

with many oscillations. The direct rational function fitting is good to be used as an interpolation tool but cannot be used in extrapolating. Figure 2.3 shows the indirect method produces the computed the S-parameters data which are both bounded and preserving the periodical nature above and below the spectrum of the measured frequencies.

The jitters in the measured S-parameter data usually comes from the instrument limitations and the human errors and requires a lot of measurements to average out. Due to the smooth nature of the S-parameter computed from the analytic equations, there is no jitter shown in the computed S-parameter. Fitting the computed S-parameter data to the measured S-parameter data will not be affected by the small measurement error jitters abundant in the examples tested.

Sometimes the measured S-parameter data can rise above 1.0 for a passive system, but with the computed S-parameters which are evaluated from the parasitic functions, they never violate the power conservation rule and hence always stable for a passive system.

The lower order moment terms in a Taylor series expansion around a given point should be order independent, which does not hold true for direct curve-fitting method. Compute S-parameter moments from parasitic functions guarantee the moment found are independent of the order of the approximation.

(a)   (b)
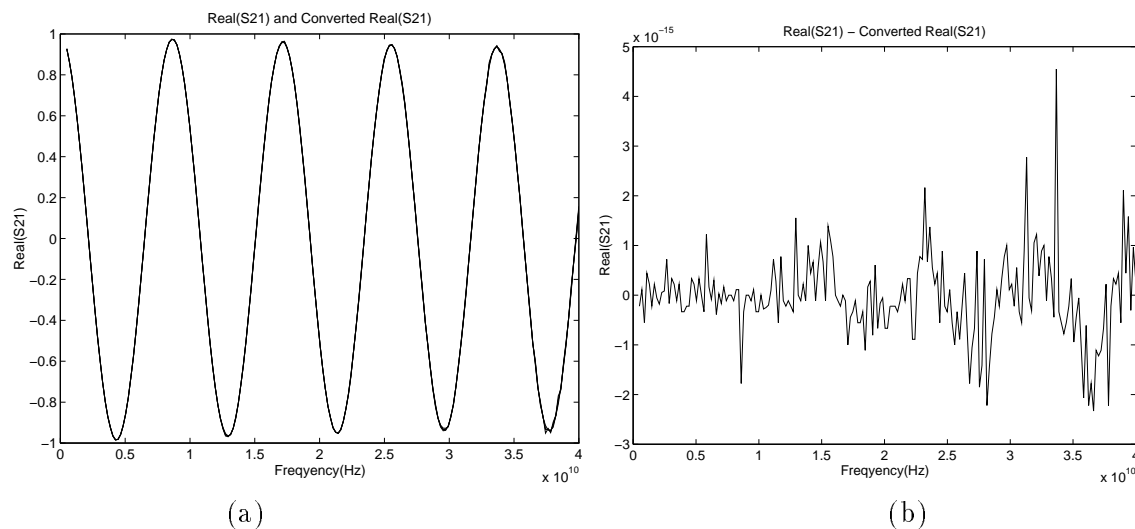
Figure 2.4: **The Introduced Conversion Error:** The original measured S-parameter data and the converted S-parameter are plotted in (a). The difference between them are plotted in (b).

The conversion processes for both the two-port measured data and $2N$-port measured data shown in Section 4 are almost lossless. The regenerated S-parameters based on the converted **RLCG** compared with the original S-parameter data show that this conversion process introduces very little error. Figure 2.4 demonstrates the conversion error is less than 10^{-15}.

3   Proposed Method of Attack

The steps required for the transient analysis of the device characterized with the measured S-parameter data macromodel include:

- Converting measured S-parameter data into parasitic functions: $\mathbf{R}(f)$, $\mathbf{L}(f)$, $\mathbf{C}(f)$ and $\mathbf{G}(f)$.

- Finding moments of the four parasitic functions through Least-Square curve-fitting of the computed S-parameter w.r.t. the measured S-parameter data.

- Computing moments of the S-parameters from the moments of the $\mathbf{R}(f)$, $\mathbf{L}(f)$, $\mathbf{C}(f)$ and $\mathbf{G}(f)$ data sets.

- Constructing macromodel for the congruence transformer for the $2N$-port coupled interconnects.

- Incorporating the computed S-parameter macromodels into the S-parameter macromodel based simulator to perform the transient analysis.

4   Converting Measured S-Parameter Data into Parasitic Functions

For the completeness of this paper, the methods for converting two-port and $2N$-port S-parameter data into the Parasitic functions are presented here.

Previous researches that converted the measured two-port S-parameter data into the **RLCG** data sets include those of Eisenstadt et al. [6] and Owazr [14]. Their primary focus was on the interconnect characterization and not on the transient simulation. Besides, only a two-port device and not the $2N$-port device was described in their papers.

The following Equations are taken from Eisenstadt et al. paper to demonstrate the steps taken to convert the S-parameters into $\mathbf{R}(f)$, $\mathbf{L}(f)$, $\mathbf{C}(f)$ and $\mathbf{G}(f)$ [6]. Starting with the S-parameter matrix of a lossy transmission line which is presented in Equation (4.1).

$$S(s) = \frac{1}{2Z_0 Z_c(s)\cosh(\gamma(s)) + (Z_c^2(s) + Z_0^2)\sinh(\gamma(s))}$$
$$\begin{bmatrix} (Z_c^2(s) - Z_0^2)\sinh(\gamma(s)) & 2Z_0 Z_c(s) \\ 2Z_0 Z_c(s) & (Z_c^2(s) - Z_0^2)\sinh(\gamma(s)) \end{bmatrix}, \tag{4.1}$$

The $Z_c(s)$ is the characteristic impedance and $\gamma(s)$ is the propagation constant. Both $Z_c(s)$ and $\gamma(s)$ are computed from the frequency-dependent values of $\mathbf{R}(f)$, $\mathbf{L}(f)$, $\mathbf{C}(f)$ and $\mathbf{G}(f)$ based on the following Equations:

$$\begin{aligned} \gamma(s) &= \sqrt{(R(s) + sL(s))(G(s) + sC(s))} \cdot l \\ Z_c(s) &= \sqrt{\frac{R(s) + sL(s)}{G(s) + sC(s)}}. \end{aligned}$$

It can be shown that:

$$e^{-\gamma l} = \left\{ \frac{1 - S_{11}^2 + S_{21}^2}{2S_{21}} \pm K \right\}^{-1}, \tag{4.2}$$

where

$$K = \left\{ \frac{(1 - S_{11}^2 + S_{21}^2)^2 - (2S_{11})^2}{(2S_{21})^2} \right\}^{\frac{1}{2}} \tag{4.3}$$

$$Z_c^2 = Z_0^2 \frac{(1 + S_{11})^2 - S_{21}^2}{(1 - S_{11})^2 - S_{21}^2}. \tag{4.4}$$

During the extraction of γ, one must choose the root with the positive attenuation factor α and correct the negative propagation β into a positive value. After extracting the γ and Z from $e^{-\gamma l}$ and Z_c^2, the $\mathbf{R}(f)$, $\mathbf{L}(f)$, $\mathbf{C}(f)$ and $\mathbf{G}(f)$ can be found from the following Equations:

$$\begin{aligned} \mathbf{R}(f) &= Re\{\gamma Z_c\} & \tag{4.5} \\ \mathbf{L}(f) &= Im\{\gamma Z_c\}/\omega & \tag{4.6} \\ \mathbf{G}(f) &= Re\{\gamma/Z_c\} & \tag{4.7} \\ \mathbf{C}(f) &= Im\{\gamma/Z_c\}/\omega. & \tag{4.8} \end{aligned}$$

The conversion for $2N$-port measured S-parameter data requires a different approach which must

handle **RLCG** matrices. Gruodis et al. has previously reported the conversion of the measured admittance and the measured impedance data into the **RLCG** data sets [9]. Applying the standard equations found in microwave textbook, one can find the admittance matrix $\mathbf{Y}_{2n}$ and impedance matrix $\mathbf{Z}_{2n}$ from the measured S-parameter data matrix $\mathbf{S}_{2n}$, and then apply Gruodis et al. method to find the parasitic function matrices: $\mathbf{R}(f)$, $\mathbf{L}(f)$, $\mathbf{C}(f)$ and $\mathbf{G}(f)$.

Assume there only exists the TEM or Quasi-TEM mode of wave propagation, for the $(n + 1)$ conductor coupled transmission lines, there are $2N$ ports. The differential equations in the frequency domain are [9]:

$$\frac{d}{dx}\left[\begin{array}{c} \mathbf{V}_S \\ \mathbf{V}_R \end{array}\right] = -\mathbf{Z}\left[\begin{array}{c} \mathbf{I}_S \\ \mathbf{I}_R \end{array}\right] \tag{4.9}$$

$$\frac{d}{dx}\left[\begin{array}{c} \mathbf{I}_S \\ \mathbf{I}_R \end{array}\right] = -\mathbf{Y}\left[\begin{array}{c} \mathbf{V}_S \\ \mathbf{V}_R \end{array}\right], \tag{4.10}$$

where $\mathbf{V}_S$ and $\mathbf{V}_R$ are the n by 1 column vector for line voltage w.r.t. the reference conductor on the sending and the receiving side, $\mathbf{I}_S$ and $\mathbf{I}_R$ are the n by 1 column vector for line current on both sides, $\mathbf{Z} = \mathbf{R} + jw\mathbf{L}$, and $\mathbf{Y} = \mathbf{G} + jw\mathbf{C}$. $\mathbf{R}(f)$, $\mathbf{L}(f)$, $\mathbf{C}(f)$ and $\mathbf{G}(f)$ are n by n symmetric matrices in which every elements are functions of frequency but independent of x.

Following the same assumptions as proposed in Gruodis et al. paper that there exists a complex square root matrix $(\mathbf{ZY})^{1/2}$, the solutions of the above differential equations become [9]:

$$\left[\begin{array}{c} \mathbf{I}_S \\ \mathbf{I}_R \end{array}\right] = \left[\begin{array}{cc} \mathbf{Y}_0 coth\mathbf{\Gamma}d & -\mathbf{Y}_0 csch\mathbf{\Gamma}d \\ -\mathbf{Y}_0 csch\mathbf{\Gamma}d & \mathbf{Y}_0 coth\mathbf{\Gamma}d \end{array}\right]\left[\begin{array}{c} \mathbf{V}_S \\ \mathbf{V}_R \end{array}\right]. \tag{4.11}$$

where

$$\mathbf{\Gamma} = (\mathbf{ZY})^{1/2} = \mathbf{P}\gamma\mathbf{P}^{-1}, \tag{4.12}$$

$$\mathbf{Y}_0 = \mathbf{Z}^{-1}\mathbf{\Gamma} = \mathbf{Y}\mathbf{\Gamma}^{-1}. \tag{4.13}$$

$\mathbf{P}$ is the eigenvector matrix of $\mathbf{\Gamma}$ as well as the eigenvector matrix of the $\mathbf{ZY}$ product, and γ is the diagonal eigenvalue matrix of $\mathbf{\Gamma}$.

Given the measured $2N$ port S-parameter data $\mathbf{S}_{2n}{}^{measd}$, the symmetry of the S-parameter matrix can be assured by taking the arithmetic average as follows:

$$\mathbf{S}_{2n} = \frac{1}{2}\left[(\mathbf{S}_{2n}{}^{measd}) + (\mathbf{S}_{2n}{}^{measd})^T\right]. \tag{4.14}$$

From any microwave text book, one can find:

$$\mathbf{Y}_{2n} = Z_0{}^{-1}([\mathbf{I}] - \mathbf{S}_{2n})([\mathbf{I}] + \mathbf{S}_{2n})^{-1} \tag{4.15}$$

$$\mathbf{Z}_{2n} = Z_0([\mathbf{I}] + \mathbf{S}_{2n})([\mathbf{I}] - \mathbf{S}_{2n})^{-1}, \tag{4.16}$$

where Z_0 is the reference impedance, and $[\mathbf{I}]$ is the identity matrix which has all elements equal to zero except the diagonal elements where they are equal to one.

After securing the $\mathbf{Y}_{2n}$ and $\mathbf{Z}_{2n}$ matrices, one can use the data analysis method 2 in Gruodis et al. paper to give [9]:

$$-\mathbf{Y}_{21}{}^{-1}\mathbf{Y}_{11} = cosh\mathbf{\Gamma}d$$

$$\mathbf{\Gamma}d = \mathbf{P}[coth^{-1}\mathbf{\Lambda}_{-\mathbf{Y}_{21}{}^{-1}\mathbf{Y}_{11}}]\mathbf{P}^{-1}, \tag{4.17}$$

where $\mathbf{P}$ is the eigenvector matrix of $-\mathbf{Y}_{21}{}^{-1}\mathbf{Y}_{11}$ as well as the eigenvector matrix of $\mathbf{\Gamma}d$. From Equations (4.17) and $\mathbf{Y}_{11} = \mathbf{Y}_0 coth\mathbf{\Gamma}d$, one has:

$$\mathbf{Y}_0 = -\mathbf{Y}_{21}sinh\mathbf{\Gamma}d$$

$$= -\mathbf{Y}_{21}\mathbf{P}[sinh(coth^{-1}\mathbf{\Lambda}_{-\mathbf{Y}_{21}{}^{-1}\mathbf{Y}_{11}})]\mathbf{P}^{-1}. \tag{4.18}$$

Having derived $\mathbf{\Gamma}d$ and $\mathbf{Y}_0$, one can use Equation (4.13) for the following:

$$\mathbf{Z} = \mathbf{R} + jw\mathbf{L} = \mathbf{\Gamma}d \cdot \mathbf{Y}_0{}^{-1} \tag{4.19}$$

$$\mathbf{Y} = \mathbf{G} + jw\mathbf{C} = \mathbf{Y}_0 \cdot \mathbf{\Gamma}d. \tag{4.20}$$

The $\mathbf{R_{ij}}$, $\mathbf{L_{ij}}$, $\mathbf{C_{ij}}$ and $\mathbf{G_{ij}}$ can be found from the following Equations:

$$\mathbf{R_{ij}}(f) = Re\{\mathbf{Z}_{ij}\} \tag{4.21}$$

$$\mathbf{L_{ij}}(f) = Im\{\mathbf{Z}_{ij}\}/\omega \tag{4.22}$$

$$\mathbf{G_{ij}}(f) = Re\{\mathbf{Y}_{ij}\} \tag{4.23}$$

$$\mathbf{C_{ij}}(f) = Im\{\mathbf{Y}_{ij}\}/\omega. \tag{4.24}$$

5 Finding the Moments of the Four Parasitic Functions

The key contribution of this paper is to find the moments of the parasitic functions indirectly. The indirect approach proposed here is to find the moments of the measured S-parameter data indirectly through converting the strongly frequency-dependent S-parameter data into parasitic functions: $\mathbf{R}(f)$, $\mathbf{L}(f)$, $\mathbf{C}(f)$ and $\mathbf{G}(f)$ data sets. When taking advantage of the fact that the $\mathbf{L}(f)$, $\mathbf{C}(f)$ and $\mathbf{G}(f)$ are weak functions of frequency and the $\mathbf{R}(f)$ is a strong function of frequency [1], the moments of these four parasitic functions are much simpler to find.

The input is the measured S-parameter data tabulated w.r.t. the sampling frequencies. The output is the moments of the parasitic functions. $\mathbf{R}(f)$, $\mathbf{L}(f)$, $\mathbf{C}(f)$ and $\mathbf{G}(f)$. These moments are the coefficients of the Taylor series expansion around $s = 0$ for the parasitic functions: First, one converts the measured S-parameter data into frequency-dependent parasitic data sets. Then a least-square curve-fitting is performed to find the coefficients of the polynomials which represent the parasitic data sets. These coefficients are used as the initial values for the following optimization procedure. The S-parameter data sets are computed from the moments of the parasitic functions based upon analytic equations. The Levenberg-Marquardt optimization method is used to find the moments of the parasitic functions through comparing the computed S-parameter and the original measured S-parameter data. The partial derivatives of the Least-Square error between these two S-parameter data sets w.r.t. each of the moments of the parasitic functions are obtained from perturbation method. Assume the initial coefficients are $C^{(0)}$, and there are total m coefficients. The next coefficients $C^{(k+1)}$ can be computed from the previous coefficients $C^{(k)}$, which according to Levenberg-Marquardt, is optimized according to the following formula [13]:

$$C^{(k+1)} = C^{(k)} - (J^T J + \lambda \Lambda)^{-1} J^T \left[\frac{\partial \, LSE}{\partial c_j} \right], \tag{5.1}$$

where k is the number of iteration, $C^{(k)}$ the column vector of the $k - th$ iteration, and LSE the Least-Square Error. J is the sensitivity matrix, J^T is the transposition vector of J where the $j - th$ element $J^T(j) = J(j)$, Λ is a value which are equal to the product of $J^T J$, and λ is the *Lagrange Multiplier* properly selected to speed up the convergence of the optimization process [13]. $J^T \left[\frac{\partial\ LSE}{\partial c_j} \right]$ represents the gradient around the current coefficients $C^{(k)}$. To obtain the sensitivity matrix J, the $j - th$ element is defined as:

$$J(j) = \frac{\partial\ LSE}{\partial c_j}, \quad 1 \le j \le m. \tag{5.2}$$

The partial derivatives are computed using a central difference method. The optimization continues until the Least-Square Error cannot be further improved, or the iteration number exceeds a preset limit. The convergence to the optimal values of Levenberg-Marquardt method is proved in [13].

6   Computing the Moments of the S-Parameter

Given the moments of the four parasitic functions $\mathbf{R}(f)$, $\mathbf{L}(f)$, $\mathbf{C}(f)$ and $\mathbf{G}(f)$, one can compute the moments of the S-parameters and create the S-parameter Macromodel to perform the transient simulation. The four parasitic functions represent the frequency-dependent losses in the measured structures.

With the assumption of quasi-TEM wave propagation, the distributions of voltages and currents in a single lossy transmission line can be described by the generalized Telegraphist's equations [3]:

$$\frac{\partial \mathbf{v}(x,t)}{\partial x} = -\mathbf{L}(f)\frac{\partial \mathbf{i}(x,t)}{\partial t} - \mathbf{R}(f)\mathbf{i}(x,t) \tag{6.1}$$

$$\frac{\partial \mathbf{i}(x,t)}{\partial x} = -\mathbf{C}(f)\frac{\partial \mathbf{v}(x,t)}{\partial t} - \mathbf{G}(f)\mathbf{v}(x,t), \tag{6.2}$$

where $0 \le x \le l$, $\mathbf{v}(x,t)$ and $\mathbf{i}(x,t)$ define the voltage distributions $v_k(x,t)$ and current distributions $i_k(x,t)$ on the conductor respectively, $\mathbf{L}(f)$ and $\mathbf{C}(f)$ are the frequency-dependent per-unit-length inductance and capacitance of the single conductor system, $\mathbf{R}(f)$ the frequency-dependent per-unit-length resistance, $\mathbf{G}(f)$ the frequency-dependent per-unit-length conductance.

In order to find the lower order approximations of $S_{11}(s)$ and $S_{21}(s)$, the representations of the

$\mathbf{R}(f)$, $\mathbf{L}(f)$, $\mathbf{C}(f)$ and $\mathbf{G}(f)$ must first be found. The method presented in Section 5 is applied to find the moments of the parasitic functions. Once found, the same moments are used to compute the lower order approximations of the S-parameters.

If one defines:

$$T(s) \quad \equiv \quad \gamma^2(s) \equiv \sum_{i=0}^{q} t_i \cdot s^i + o(s^q) \tag{6.3}$$

$$A(s) \quad \equiv \quad Z_c(s)\gamma(s) - Z_0^2 \cdot \frac{\gamma(s)}{Z_c(s)} \equiv \sum_{i=0}^{q} a_i \cdot s^i + o(s^q) \tag{6.4}$$

$$B(s) \quad \equiv \quad Z_c(s)\gamma(s) + Z_0^2 \cdot \frac{\gamma(s)}{Z_c(s)} \equiv \sum_{i=0}^{q} b_i \cdot s^i + o(s^q), \tag{6.5}$$

whereas $\gamma^2(s) = (R(s)+sL(s))(G(s)+sC(s))$, $\frac{\gamma(s)}{Z_c(s)} = G(s)+sC(s)$, and $Z_c(s)\gamma(s) = R(s)+sL(s)$. There is no square root involved in the evaluation of the approximations of the $T(s)$, $A(s)$, and $B(s)$ complex functions. The approximation of the $R(s)$, $L(s)$, $G(s)$, and $C(s)$ real functions are known through *indirect* curve-fitting. The coefficients of the $T(s)$, $A(s)$, and $B(s)$ complex functions can be found through simple polynomial operations.

If one separates the constant term from the rest of the function,

$$T(s) \quad \equiv \quad t_0 + \sum_{i=1}^{q} t_i \cdot s^i + o(s^q) \equiv t_0 + T_q(s) + o(s^q). \tag{6.6}$$

It will make the finding of the coefficients in Equation (6.11) and (6.12) much easier. The expansions of $2Z_0 \cosh(\gamma(s))$ and $\frac{\sinh(\gamma(s))}{\gamma(s)}$ are shown in Equation (6.7) and (6.8):

$$U(s) \quad \equiv \quad 2Z_0 \cosh(\gamma(s)) \equiv \sum_{i=0}^{\infty} \frac{\gamma^{2i}(s)}{2i!} \equiv 2Z_0 \sum_{i=0}^{\infty} \frac{T^i(s)}{2i!} \equiv 2Z_0 \sum_{i=0}^{q} u_i \cdot s^i + o(s^q) \tag{6.7}$$

$$V(s) \quad \equiv \quad \frac{\sinh(\gamma(s))}{\gamma(s)} \equiv \sum_{i=0}^{\infty} \frac{\gamma^{2i}(s)}{(2i+1)!} \equiv \sum_{i=0}^{\infty} \frac{T^i(s)}{(2i+1)!} \equiv \sum_{i=0}^{q} v_i \cdot s^i + o(s^q). \tag{6.8}$$

Based on Equations (6.4), (6.5), (6.7), and (6.8), the representations of $S11$ and $S21$ can be rewritten as:

$$S_{11}(s) \quad = \quad \frac{A(s) \cdot V(s)}{U(s) + B(s) \cdot V(s)} \tag{6.9}$$

$$S_{21}(s) = \frac{2Z_0}{U(s) + B(s) \cdot V(s)}. \tag{6.10}$$

It can be shown that:

$$U(s) = 2Z_0 \sum_{k=0}^{q} \beta_k \cdot T_q^k(s) + o(s^q) \tag{6.11}$$

$$V(s) = \sum_{k=0}^{q} \alpha_k \cdot T_q^k(s) + o(s^q), \tag{6.12}$$

where

$$\beta_k = \sum_{k=0}^{\infty} \frac{C_i^k}{2i!} \cdot t_0^{i-k} \tag{6.13}$$

$$\alpha_k = \sum_{k=0}^{\infty} \frac{C_i'^k}{(2i+1)!} \cdot t_0^{i-k}, \tag{6.14}$$

and t_0 is the separated constant term in Equation (6.6). Although the summation of both α_k and β_k are an infinity series, in reality, the inverse of the factorial is a fast converging series and they can be truncated at a certain point without introducing much error. The coefficients of $U(s)$ and $V(s)$ are:

$$u_i = \sum_{k=1}^{i} \beta_k \sum_{j_1 + j_2 + \cdots + j_k = i} t_{j_1} \cdot t_{j_2} \cdots t_{j_k} \tag{6.15}$$

$$v_i = \sum_{k=1}^{i} \alpha_k \sum_{j_1 + j_2 + \cdots + j_k = i} t_{j_1} \cdot t_{j_2} \cdots t_{j_k}. \tag{6.16}$$

Since the coefficients of the polynomial $T(s)$ are known from Equation (6.3), the coefficients of $U(s)$ and $V(s)$ can then be computed.

If one defines:

$$S_{11}(s) = \frac{C(s)}{D(s)} \tag{6.17}$$

$$S_{21}(s) = \frac{C'(s)}{D(s)}. \tag{6.18}$$

Comparing Equations (6.9), (6.10), (6.17), and (6.18), one finds:

$$C(s) \equiv \sum_{i=0}^{q} c_i \cdot s^i + o(s^q) = A(s) \cdot V(s) \tag{6.19}$$

$$D(s) \equiv \sum_{i=0}^{q} d_i \cdot s^i + o(s^q) = U(s) + B(s) \cdot V(s) \tag{6.20}$$

$$C'(s) = 2Z_0. \tag{6.21}$$

It can be shown that the coefficients of $C(s)$ and $D(s)$ are:

$$c_k = \sum_{i+j=k} a_i v_j \tag{6.22}$$

$$d_k = u_k + \sum_{i+j=k} b_i v_j. \tag{6.23}$$

If the moments of $S_{11}(s)$ and $S_{21}(s)$ are m_i and n_i respectively, one can write:

$$S_{11}(s) = \sum_{i=0}^{q} m_i \cdot s^i + o(s^q) \tag{6.24}$$

$$S_{21}(s) = \sum_{i=0}^{q} n_i \cdot s^i + o(s^q). \tag{6.25}$$

From Equation (6.17) and (6.25), one can derive:

$$\sum_{i+j=k} m_i d_j = c_k. \tag{6.26}$$

If one denotes:

$$D_q = \begin{bmatrix} d_0 & 0 & 0 & \ldots & 0 \\ d_1 & d_0 & 0 & \ldots & 0 \\ d_2 & d_1 & d_0 & \ldots & 0 \\ \ldots & & & & \\ d_q & d_{q-1} & d_{q-2} & \ldots & d_0 \end{bmatrix} \tag{6.27}$$

$$M_q = \begin{bmatrix} m_0 & m_1 & m_2 & \cdot & \cdot & \cdot & m_q \end{bmatrix}^T \tag{6.28}$$

$$C_q = \begin{bmatrix} c_0 & c_1 & c_2 & \cdot & \cdot & \cdot & c_q \end{bmatrix}^T, \tag{6.29}$$

where T represents the transpose of the vector, one can rewrite $D_q M_q = C_q$, i.e. $M_q = D_q^{-1} C_q$. Thus the moments m_i of the $S_{11}(s)$ function can be found through simple backward substitutions. Similarly, if one denotes:

$$N_q = \begin{bmatrix} n_0 & n_1 & n_2 & \cdot & \cdot & \cdot & n_q \end{bmatrix}^T \tag{6.30}$$

$$C_q' = \begin{bmatrix} 2Z_0 & 0 & 0 & \cdot & \cdot & \cdot & 0 \end{bmatrix}^T, \tag{6.31}$$

where T again represents the transpose of the vector, one can rewrite $D_q N_q = C_q'$, i.e. $N_q = D_q^{-1} C_q'$, and the moments n_i of the $S_{21}(s)$ function can again be found through simple backward substitutions.

Once the moments of the $S11$ and $S21$ of the two-port interconnect are established, they are passed to the S-parameter macromodel based simulator to perform the transient analysis.

The analysis of $2N$-port coupled interconnects are different from that of the two-port interconnect analysis. However, after decoupling, the $2N$-port coupled interconnects analysis becomes that of the decoupling congruence transformers and that of the decoupled two-port interconnects [19].

Starting from the assumption of quasi-TEM wave propagation, the distributions of voltages and currents in a n coupled lossy transmission-line system can be described by the generalized Telegraphist's equations [3]:

$$\frac{\partial \mathbf{v}(x,t)}{\partial x} = -\mathbf{L}(\mathbf{f})\frac{\partial \mathbf{i}(x,t)}{\partial t} - \mathbf{R}(\mathbf{f})\mathbf{i}(x,t) \tag{6.32}$$

$$\frac{\partial \mathbf{i}(x,t)}{\partial x} = -\mathbf{C}(\mathbf{f})\frac{\partial \mathbf{v}(x,t)}{\partial t} - \mathbf{G}(\mathbf{f})\mathbf{v}(x,t), \tag{6.33}$$

where $0 \leq x \leq l$, $\mathbf{v}(x,t)$ and $\mathbf{i}(x,t)$ are column vectors defining the voltages distributions $v_k(x,t)$ and currents distributions $i_k(x,t)$ on the conductors $k = 1,2,3,...,n$, $\mathbf{L}(\mathbf{f})$ and $\mathbf{C}(\mathbf{f})$ are the n by n symmetric matrices of the frequency-dependent per-unit-length inductance and capacitance of the n conductor system respectively, $\mathbf{R}(\mathbf{f}) = diag(R_{kk}(f))$, $k = 1...n$ the diagonal matrix of the frequency-dependent per-unit-length resistance, $\mathbf{G}(\mathbf{f})$ the n by n symmetric matrix of the frequency-dependent per-unit-length conductance [16].

To incorporate the macromodel of the frequency-dependent decoupling networks into the S-

parameter macromodel simulator presents a challenge. This process requires the finding of a frequency-dependent transformation matrix in order to decouple the system. It is a complex process and requires the eigenvalues at each frequency point prior to diagonalization. The resulting matrix elements are characterized by the tabulated S-parameter data.

Taking the Laplace transform of the Equation (6.32) and (6.33), they can be rewritten as:

$$\frac{\partial \mathbf{V}(x,s)}{\partial x} \quad = \quad -\mathbf{ZI}(x,s) \tag{6.34}$$

$$\frac{\partial \mathbf{I}(x,s)}{\partial x} \quad = \quad -\mathbf{YV}(x,s), \tag{6.35}$$

where $\mathbf{Z} = \mathbf{R} + jw\mathbf{L}$, and $\mathbf{Y} = \mathbf{G} + jw\mathbf{C}$. Throughout this paper, the following assumptions reported by Blazeck et al. are used [2]. The modes of propagation must be TEM or quasi-TEM, and the lines are of uniform cross-section throughout their length; that is, $\mathbf{R}$, $\mathbf{L}$, $\mathbf{C}$, and $\mathbf{G}$ are assumed to be constant with respect to the spatial variable x.

Solving Equation (6.34) and (6.35), one has:

$$\frac{\partial^2 \mathbf{V}(x,s)}{\partial x^2} \quad = \quad \mathbf{ZYV}(x,s) = \mathbf{\Gamma}^2 \mathbf{V}(x,s) \tag{6.36}$$

$$\frac{\partial^2 \mathbf{I}(x,s)}{\partial x^2} \quad = \quad \mathbf{YZI}(x,s) = (\mathbf{\Gamma}^2)^T \mathbf{I}(x,s), \tag{6.37}$$

where T indicates transpose and $\mathbf{\Gamma}$ defined as $\mathbf{\Gamma}^2 = \mathbf{ZY}$ [2]. The existence of eigenvectors that diagonalize $\mathbf{\Gamma}^2$ and $\mathbf{\Gamma}$ is also assumed throughout this paper [2]. Define

$$\mathbf{\Gamma} = \mathbf{X\Lambda X}^{-1}, \tag{6.38}$$

where $\mathbf{X}$ is the eigenvectors of $\mathbf{\Gamma}$; therefore, they are also the eigenvectors of $\mathbf{\Gamma}^2$, and $\mathbf{\Lambda}$ is the diagonal matrix of the eigenvalues of $\mathbf{\Gamma}$. It can be shown that [5]

$$\frac{\partial \mathbf{V_m}(x,s)}{\partial x} \quad = \quad -\mathbf{\Lambda Z_m I_m}(x,s) \tag{6.39}$$

$$\frac{\partial \mathbf{I_m}(x,s)}{\partial x} \quad = \quad -\mathbf{\Lambda Y_m V_m}(x,s), \tag{6.40}$$

where $\mathbf{V}(x,s) = \mathbf{XV_m}(x,s)$, $\mathbf{I}(x,s) = (\mathbf{X}^T)^{-1}\mathbf{I_m}(x,s)$. The modal impedance matrix $\mathbf{Z_m}$ and

modal admittance matrix $\mathbf{Y_m}$ are related to the eigenvector matrix $\mathbf{X}$ and the impedance matrix $\mathbf{Z}$ by

$$\mathbf{Z_m} = (\mathbf{Y_m})^{-1} = \mathbf{\Lambda}^{-1}\mathbf{X}\mathbf{Z}(\mathbf{X}^T)^{-1}. \tag{6.41}$$

With the eigenvector matrix $\mathbf{X}$, the original coupled transmission lines can be decoupled into two congruence transformers and a set of n decoupled transmission lines [3]. The task of finding the macromodel of the frequency-dependent coupled transmission lines becomes that of finding the macromodel representations of the congruence transformers and the frequency-dependent single transmission lines. The macromodel of the single transmission line characterized with frequency-dependent losses has already been developed in the early part of this section. The remaining task is to find the macromodel representation of a frequency-dependent congruence transformer.

It can be shown that for the coupled lossy transmission line systems, the congruence transformer matrix is the eigenvector matrix of the complex matrix $\mathbf{\Gamma}$ [2]. The existence of such eigenvector matrix $\mathbf{X}$ that simultaneously diagonalize the complex matrices $\mathbf{\Gamma}$, $\mathbf{\Gamma}^2$, $\mathbf{ZY}$, and $\mathbf{YZ}$ is assumed throughout this paper. This assumption is also adopted by Gordon et al. [8], Blazeck et al. [2] and Schutt-Aine et al. [16].

Gordon et al. suggested that the frequency-dependent congruence transformer can be found by performing the congruence decoupling at each frequency point, as well as by checking the orthogonality of all the eigenvectors for all the frequency points [8]. If the eigenvectors were not orthogonal to each other, column swapping must be performed so that for all the congruence transformation matrices at all the frequency points are orthogonal to any other one. During this process, the $\mathbf{R}(f)$, $\mathbf{L}(f)$, $\mathbf{C}(f)$ and $\mathbf{G}(f)$ matrices have been diagonalized to be: $diag(\mathbf{R}(f))$, $diag(\mathbf{L}(f))$, $diag(\mathbf{C}(f))$ and $diag(\mathbf{G}(f))$ eigenvalue matrices. The $i - th$ diagonal eigenvalues of each frequency points constitute the parasitic functions of the decoupled frequency-dependent single transmission line. Thus these diagonal eigenvalue matrices can be used to form the macromodels using a method outlined in the early part of this Section.

Once the tabulated S-parameter data for the congruence transformation have been found, a curve-fitting using Levenberg-Marquardt method [13] is used to find the moments for the construction of the congruence transformer: $X(f)$.

- the HP Spice simulator from Hewlett Packard Company.

- the S-parameter Macromodel based simulator.

Throughout all the examples, the simulation waveforms of the HP Spice serve as the correct solutions, because its underlying implementation is the direct convolution. The direct convolution with the impulse response obtained through IFFT method is considered to be the most accurate method for the transient analysis of the frequency-dependent transmission lines because there is no approximation involved [18] [7]. The only drawback is the simulation time is exponentially proportioned to the transient analysis time[8].

All the results show that the output waveforms of the measured S-parameter macromodel match well with those produced by HP Spice simulator as expected. The seemly differences that were shown on both the near end and far end waveforms are due to the lower order chosen and the Pade approximation error. In all the examples, increase the order of Pade approximation does not increase accuracy, one must turn to other method such as the Pade-via-Lancsoz (PVL) the to solve this accuracy problem.

7.1   Example 1

This is an example with two uniform transmission line sections each with different width joined together, and the whole structure is characterized with measured S-parameter data. It is simulated using the same test circuit and input driving signal. The near end and far end simulation waveforms of the HP Spice simulator and the S-parameter macromodel based simulator are shown in Figure 7.2 (a) and Figure 7.2 (b) respectively.   Figure 7.3 shows enlarged waveforms.

7.2   Example 2

This is an example with an uniform transmission line characterized with measured S-parameter data. It is simulated using the same test circuit and input driving signal. The near end and far end simulation waveforms of the HP Spice simulator and the S-parameter macromodel based simulator are shown in Figure 7.4 (a) and Figure 7.4 (b) respectively.
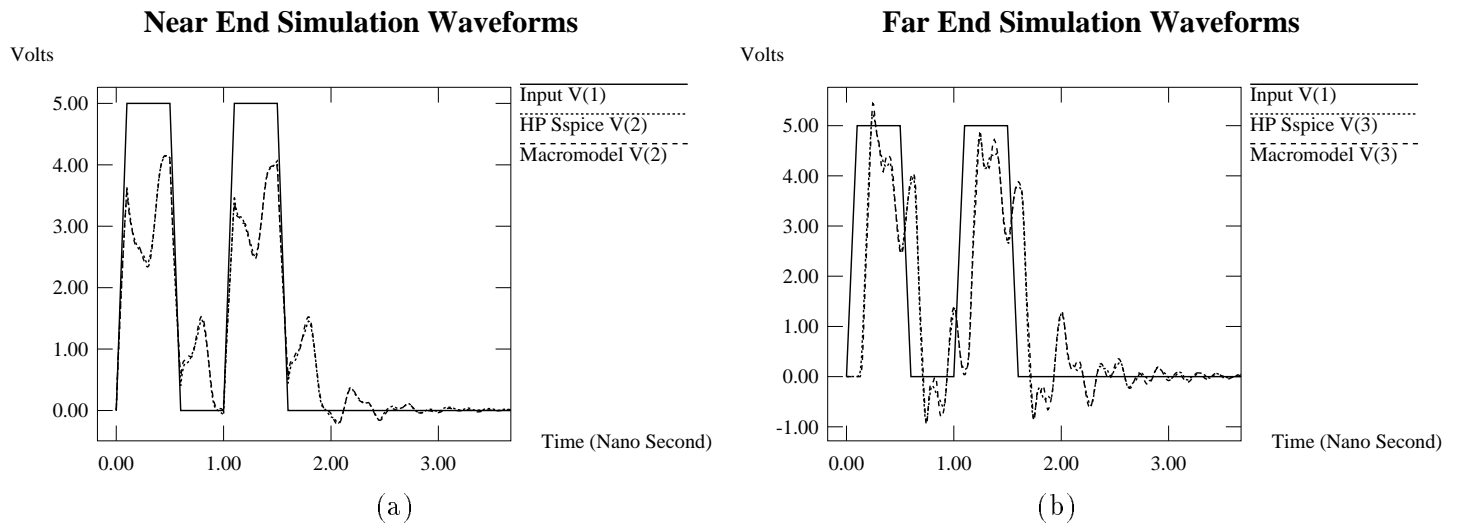
Near End Simulation Waveforms

Volts

Input V(1)
HP Sspice V(2)
Macromodel V(2)

5.00
4.00
3.00
2.00
1.00
0.00

Time (Nano Second)

0.00   1.00   2.00   3.00

(a)

Far End Simulation Waveforms

Volts

Input V(1)
HP Sspice V(3)
Macromodel V(3)

5.00
4.00
3.00
2.00
1.00
0.00
-1.00

Time (Nano Second)

0.00   1.00   2.00   3.00

(b)

Figure 7.2: **Simulation Waveforms of the Transmission Line characterized with measured S-parameter data:** The output waveforms of the near end of the two-port is shown in (a), waveforms of the far end of the two-port is shown in (b).

Far End Simulation Waveforms

Volts

HP Sspice V(3)
Macromodel V(3)

1.50

1.00

0.50

0.00

-0.50

Time (Nano Second)
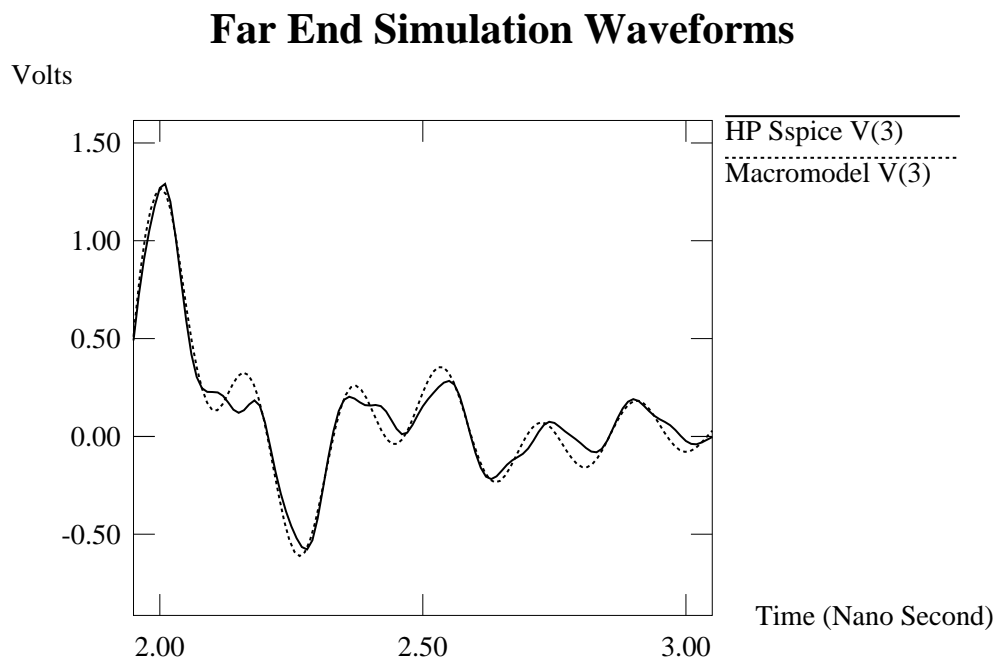
2.00   2.50   3.00

Figure 7.3: **Enlarged Far End Simulation Waveforms:** The two closely follow each other are the simulation waveforms of the HP Spice and the S-parameter based Macromodel simulator.

Near End Simulation Waveforms

(a)

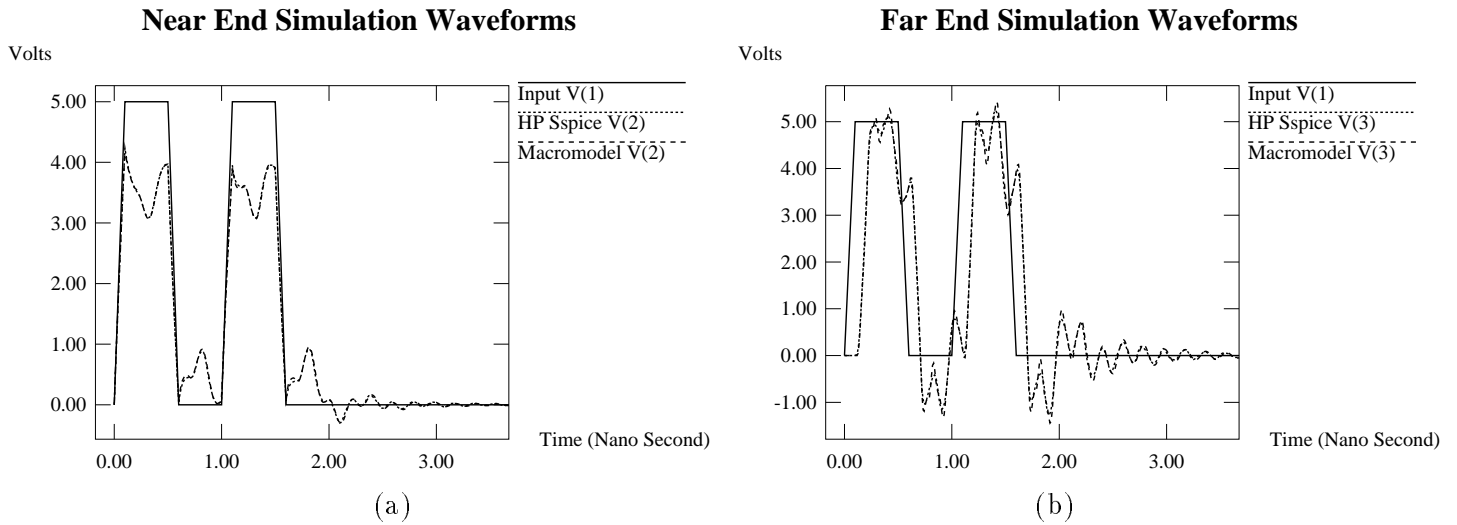**Far End Simulation Waveforms**

(b)

Figure 7.4: **Simulation Waveforms of the Transmission Line characterized with measured S-parameter data:** The output waveforms of the near end of the two-port is shown in (a), waveforms of the far end of the two-port is shown in (b).

7.3   Example 3

This is an example with two uniform transmission line sections joined by a 90^0 bend, and the whole structure is characterized with measured S-parameter data. It is simulated using the same test circuit and input driving signal. The near end and far end simulation waveforms of the HP Spice simulator and the S-parameter macromodel based simulator are shown in Figure 7.5 (a) and Figure 7.5 (b) respectively.

8   Conclusions

Designing interconnect networks for today's high performance digital systems requires more accurate and more efficient transient analysis of the interconnects characterized by the measured S-parameter data. The novel macromodel of transmission lines and discontinuities characterized by the measured S-parameter data is developed.

The main contribution of this paper is an indirect method for finding the moments from the measured S-parameter data. This indirect approach produces more accurate moments than those obtained from fitting the S-parameter directly. It also capture the periodical nature of the S-parameters in the frequency spectra both above and below the sampled frequency points.

Near End Simulation Waveforms

Far End Simulation Waveforms

Volts

Volts

Input V(1)
HP Sspice V(2)
Macromodel V(2)

Input V(1)
HP Sspice V(3)
Macromodel V(3)

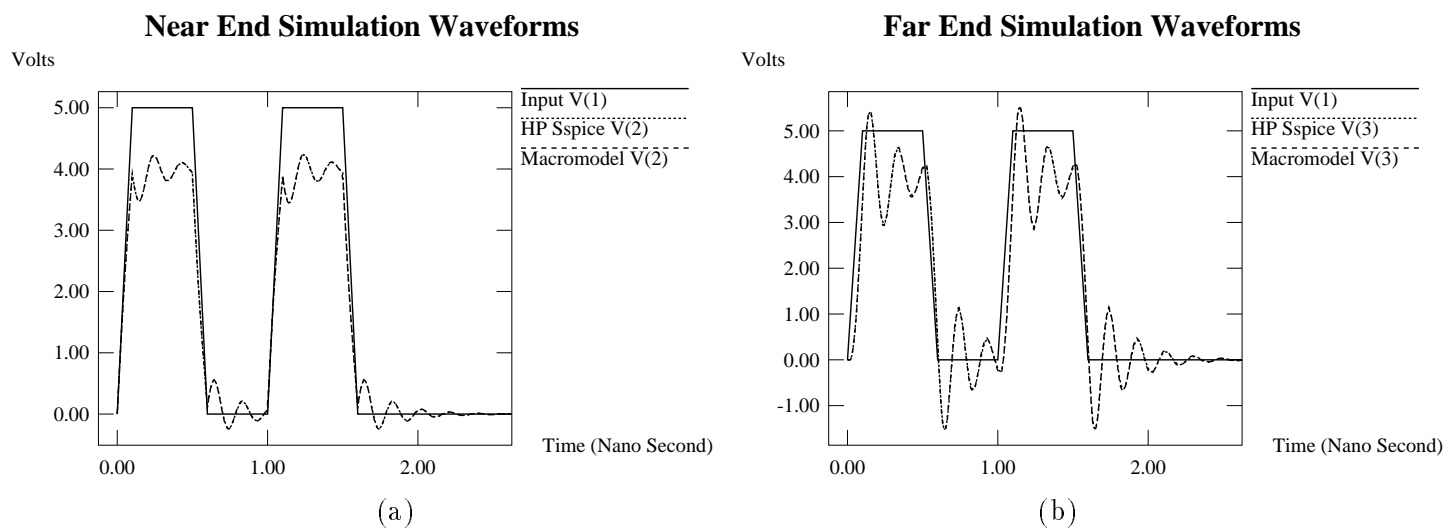Time (Nano Second)

Time (Nano Second)

(a)

(b)

Figure 7.5: **Simulation Waveforms of the Transmission Line characterized with measured S-parameter data:** The output waveforms of the near end of the two-port is shown in (a), waveforms of the far end of the two-port is shown in (b).

Furthermore, the moments produced are independent of the approximation order which usually does not hold true for the curve-fitting methods. Since the moments are computed from the four parasitic functions, they observe power conservation rule for passive system. By the same token, the computed S-parameters are smooth functions of frequency, and this makes this indirect approach insensitive to measurement errors. The results in Section 7 show very good agreements with the results produced by the direct convolution approach implemented in the HP Spice.

9   Acknowledgments

References

[1] C. E. Baumgartner. *Simulation methods for multi-conductor transmission lines in electronic applications*. PhD thesis, University of Arizona, Tuson, 1992.

[2] Thomas S. Blazeck and Raj Mittra. Transient analysis of lossy multiconductor transmission lines in nonlinear circuits. *IEEE Trans. on Components, Hybrids and Manufacturing Technology*, CHMT-14(3):618–627, 1991.

[3] F.Y. Chang. The generalized method of characteristic for waveform relaxation analysis of lossy coupled transmission lines. *IEEE Trans. on Microwave Theory and Techniques*, MTT-37, No. 12:2028–2038, 1989.

[4] Norman H. J. Chang. Rational function curve-fitting for the transient analysis of measured s-parameter data. Private communication, 1995.

[5] Tom Dhaene and Daniel De Zutter. Selection of lumped element models for coupled lossy transmission lines. *IEEE Trans. on Computer-Aided Design*, 11(7):805,815, July 1992.

[6] William R. Eisenstadt and Yungseon Eo. S-parameter-based IC interconnect transmission line characterization. *IEEE Trans. on Components, Hybrids and Manufacturing Technology*, CHMT-15(4):483–490, August 1992.

[7] David S. Gao, Andrew T. Yang, and Sung Mo Kang. Modeling and simulation of interconnect delays and crosstalks in high-speed integrated circuits. *IEEE Trans. on Circuits and Systems*, Vol. 37:1–9, January 1990.

[8] Colin Gordon, Thomas Blazeck, and Raj Mittra. Time-domain simulation of multiconductor transmission lines with frequency-dependent losses. *IEEE Trans. on Computer-Aided Design*, 11(11):1372–1387, Novenber 1992.

[9] C. S. Gruodis and A. J. Chang. Coupled lossy transmission line characterization and simulation. *IBM J. Res. Develop*, 25(1):25–41, January 1981.

[10] Rongxiang Julie Hu and Ernest S. Kuh. Integrating networks characterized by measured s-parameter data into swec. Technical Report Memorandum No. UCB/ERL M94/68, University of Clifornia, Berkeley, Aug. 1994.

[11] Dmitri Kuznetsov and Jose Schutt-Aine. The optimal transient simulation of distributed lines, Part I: formulation of the optimal method. Submitted for publication in IEEE Trans. of Circuits and Systems Fundamental Theory and Applications.

[12] Dmitri Kuznetsov and Jose Schutt-Aine. The optimal transient simulation of distributed lines, Part II: Difference approximation. Submitted for publication in IEEE Trans. of Circuits and Systems Fundamental Theory and Applications.

[13] D. W. Marquardt. An algorithm for least-squares estimation of nonlinear parameters. *Journal of Society of Indust. Appl. Math.*, 11:431–441, 1963.

[14] Amir Owazr, M. Wickhmann, and M. Kasper. Line parameter characterization of laser deposited lines. In *Proc. of IEEE EPEP-94*, November 1994.

[15] R. Sanaie, Eli Chiprout, Michel S. Nakhla, and Qi-Jun Zhang. Integrating subnetworks characterized by measured data into moment-matching simulations. In *Proc. of IEEE Multi-Chip Module Conference MCMC-94*, pages 114–119, 1994.

[16] Jose E. Schutt-Aine and Raj Mittra. Nonlinear transient analysis of coupled transmission lines. *IEEE Trans. on Microwave Theory and Techniques*, MTT-36, No. 7:959–966, 1989.

[17] L. Miguel Silveria, Ibrahim M. Elfadel, and Jacob K. White. An efficient approach to transmission line simulation using measured of tabulated s-parameter data. *31st th ACM/IEEE Design Automation Conference Proceedings*, pages 634–639, 1994.

[18] Boris Troyanovsky and Norman H. J. Chang. Hp Sspice user manual. Private communication, 1994.

[19] Jimmy Wang and Wayne Dai. Transient analysis of coupled transmission lines using scattering parameter based macromodel. Technical Report UCSC-CRL-94-09, University of Clifornia, Santa Cruz, 1994.